Title

Observation of Return Current Effects in a Passive Plasma Lens

Permalink

Authors

Govil, R
Leemans, W P
Backhaus, E Yu
et al.

Publication Date

1999-03-01

LBNL-43093
Preprint

ERNEST ORLANDO LAWRENCE BERKELEY NATIONAL LABORATORY

Observation of Return Current Effects in a Passive Plasma Lens

R. Govil, W.P. Leemans, E. Yu Backhaus, and J.S. Wurtele

Accelerator and Fusion Research Division

March 1999

Submitted to
Physical Review Letters

LBNL-43093
CBP Note-289

Observation of Return Current Effects in a Passive Plasma Lens*

R. Govil and W.P. Leemans
Center for Beam Physics
Lawrence Berkeley National Laboratory
Berkeley, California 94720

E. Yu Backhaus and J. S. Wurtele
Physics Department
University of California at Berkeley
Berkeley, California 94720

March 25, 1999

Submitted to *Physical Review Letters*

* This work was supported by the Director, Office of Energy Research, Office of High Energy and Nuclear Physics, High Energy Physics Division, of the U. S. Department of Energy, under Contract No. DE-AC03-76SF00098.

Observation of return current effects in a passive plasma lens

R. Govil and W.P. Leemans

Center for Beam Physics, Lawrence Berkeley National Laboratory, Berkeley, CA 94720

E. Yu. Backhaus and J.S. Wurtele

Physics Dept., University of California at Berkeley, Berkeley, CA 94720

(March 25, 1999)

Abstract

Observations of relavistic beam focusing by a passive plasma lens have demonstrated a reduction in focusing strength due to plasma return current. A 50MeV beam was propagated through a 1-3 cm long plasma with density around 10^{14} cm^{-3}. Beam size was measured as a function of propagation distance. For a ratio of collisionless plasma skindepth to beam spot size $k_p\sigma_r$ =0.33, no significant reduction in focusing was observed. Reduced focusing was measured for $k_p\sigma_r = 1.1$, where a significant fraction of the inductively driven return current in the plasma flows within the beam. The observations are in good agreement with an envelope equation model and with particle-in-cell simulations.

Typeset using REVTEX

The high electric fields that can be attained in plasmas have generated much interest for acceleration [1], focusing [2] and transport of particle beams. Next generation linear colliders require strongly focused beams to achieve the desired high luminosity [3]. Plasma lenses hold the promise of providing focusing strength on the order of 3-10 MG/cm. This is several orders of magnitude larger than can be produced by current day conventional magnets.

The physical mechanism for focusing of particle beams by passive (no external current) plasmas is the expulsion of plasma electrons from the area occupied by the beam and the focusing of the beam in the net plasma and beam fields. The behavior of the lens can be characterized by the ratio of plasma density n_p to beam density n_b. In an overdense plasma lens where $n_p >> n_b$, the space-charge of the electron beam is fully neutralized by the plasma through the displacement of plasma electrons by the beam electrons, resulting in beam self-focusing through its own magnetic field [4]. In the underdense lens, where $n_p << n_b$, all plasma electrons are displaced by the beam electrons, and the focusing force is due to the remaining plasma ions [5].

In addition to radial charge displacement, the changing magnetic flux of a bunch induces a longitudinal return current in the plasma which, by Lenz' law, will flow in the opposite direction to the beam current. The scalength for the radius over which the plasma return current flows is on the order of $c/\omega_p \equiv k_p^{-1}$, where c is the speed of light, $\omega_p = \sqrt{e^2 n_0 / m\epsilon_0}$ is the plasma frequency, n_0 the plasma density, m is the electron rest mass and ϵ_0 is the dielectric constant. As discussed below, in the overdense regime, the radial force acting on the electron beam is determined by the net current density (the difference between the beam and plasma return current density). Return current effects on the propagation of electron beams in plasmas should therefore become important when the electron beam size, σ_r, is comparable to or greater than the collisionless plasma skindepth, i.e. $k_p\sigma_r \geq 1$, and should lead to a significant reduction in net current. Previous work has observed focusing in the regime where return current is not significant [4].

The reduction in focusing caused by the plasma return current can be at times highly desirable. For example, very overdense plasma lenses have been proposed to suppress beamstrahlung [6] during the beam-beam interaction in a high energy collider. Intense low energy beam propagation in plasmas is important for the fast ignitor scheme [7] for plasma fusion. Here, ultra-high current (> MA), low energy electron beams, generated by the interaction of an intense laser pulse with a plasma, have been suggested as a means of depositing large amounts of energy into compressed, ultra-high density fusion targets. Currents much larger than the Alfven current, $I_A = mc^3/e = 17.1kA$, are needed to achieve proper fusion conditions. The propagation of such intense high current beams through high density plasmas [8] is therefore expected to rely on significant current neutralization by the surrounding plasma.

In this Letter we report results [9] of an experimental study of return current cancellation in overdense plasmas through its effect on beam focusing, and a detailed comparison with analytical and particle-in-cell code modeling. The experiments were performed at the Beam Test Facility (BTF) [10] at Lawrence Berkeley National Laboratory (LBNL). The experimental setup is shown in Fig.1.

Electron bunches with energy of 50 MeV (energy spread $0.2 - 0.4\%$) containing typically 1.3 nC of charge within a 10-15 ps (rms) bunch length, were produced by the linear accelerator (linac) injector of the LBNL Advanced Light Source (ALS). The linac consists of a thermionic gun operated at 120 kV which produces a 2 ns long electron bunch, three radio-frequency (RF) buncher cavities (125 MHz, 500 MHz and 3 GHz) that compress the pulse to about 30 ps and two 3 GHz accelerator structures which accelerate the electrons to an energy of 50 MeV. Bend magnets and quadrupoles (BTF line) transported the beam to a 1.2 m long interaction chamber, which was separated from the transport line by a 7 μm thick kapton window to allow for high pressures in the chamber. The transport efficiency of the line was optimized by appropriately tuning the magnet settings while monitoring the charge per bunch detected using integrating current transformers, labeled ICT in Fig.1, located at the exit of the linac, before the final quadrupole doublet focusing magnets and inside the vacuum chamber, respectively.

FIGURES

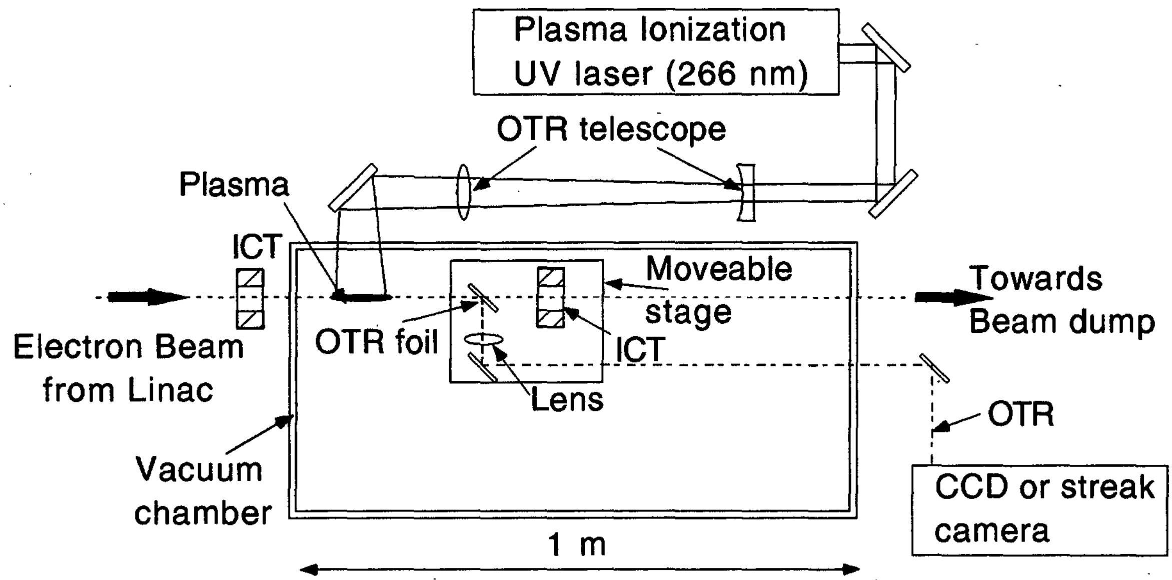

FIG. 1. Experimental setup for the plasma lens experiment. The vacuum chamber is isolated from the beamline with a 7 μm thick kapton window and is filled with TPA vapor during plasma lens experiments.

The electron beam profile was monitored inside the chamber using a scanning optical transition radiation (OTR) system [11]. Backward OTR [12], produced when the electron beam hit an aluminum coated fused silica mirror, was collected with a 50 mm diameter, 170 mm focal length lens. The OTR mirror, collection optics and an ICT were mounted on a 1 m long motorized translation stage. Detailed measurements of the beam size as a function of propagation distance were made by changing the downstream position of the OTR diagnostic setup. After exiting the chamber, the OTR was transported through an 8 m long telescope, providing an image of the electron beam at the radiator location onto a high resolution, 16 bit charge-coupled device (CCD) camera, or on a streak camera with 1.2 ps (rms) temporal resolution. The CCD camera and streak camera were used to measure the time-integrated beam profile as a function of distance and bunch length, respectively. To maintain constant magnification, pathlengths between lenses were automatically compensated when the internal stage was scanned. The imaging resolution was 16 μm.

The unnormalized rms beam emittance ϵ, measured with the OTR scanning system for a fixed quadrupole magnet setting, was 0.3 - 0.5 mm-mrad (rms), where the range was due to day-to-day variations in accelerator control settings and ensuing magnetic lattice changes. Bunch duration σ_z (rms), was on the order of 10-15 ps.

Plasmas were produced by laser based two-photon ionization of tripropylamine (TPA) with a frequency quadrupled Nd:YAG laser (266 nm) [16]. The laser beam was focused to a line focus with a spot size on the order of 1 mm high and 1-2 cm wide, using cylindrical lenses at 90^0 with respect to the electron beam. This geometry allows control over the longitudinal and transverse plasma density profile. After an initial pump-down, the vacuum chamber was filled with TPA vapor up to the vapor pressure (3.6 Torr at room temperature). The plasma density was measured using an in-quadrature 94.3 GHz microwave Mach-Zehnder interferometer, capable of providing both phase shift and amplitude variation of the microwave signal through the plasma simultaneously. The microwave beam propagated through the 1 mm thin plasma, orthogonally to the laser beam and electron beam. For laser intensities up to 150 MW/cm^2 and pressures up to the vapor pressure, the plasma density was found to scale linearly with TPA pressure and quadratically with laser intensity. Densities as high as 5×10^{14} cm^{-3} were measured. The measurement of plasma densities higher than the critical density was made possible by detection of the evanescent waves through the finite size plasma (thinner than the microwave skindepth), using the in-quadrature method [16].

Figure 2 shows an example of the change in electron beam shape due to plasma focusing, at a given position inside the experimental chamber (a) without any TPA and (b) with 4.1 Torr laser ionized TPA. The laser produced plasma length was about 1.7 cm with a density of about 2×10^{14} cm^{-3}. The reduction in beam size and increase in intensity are clear indications of plasma lens focusing.

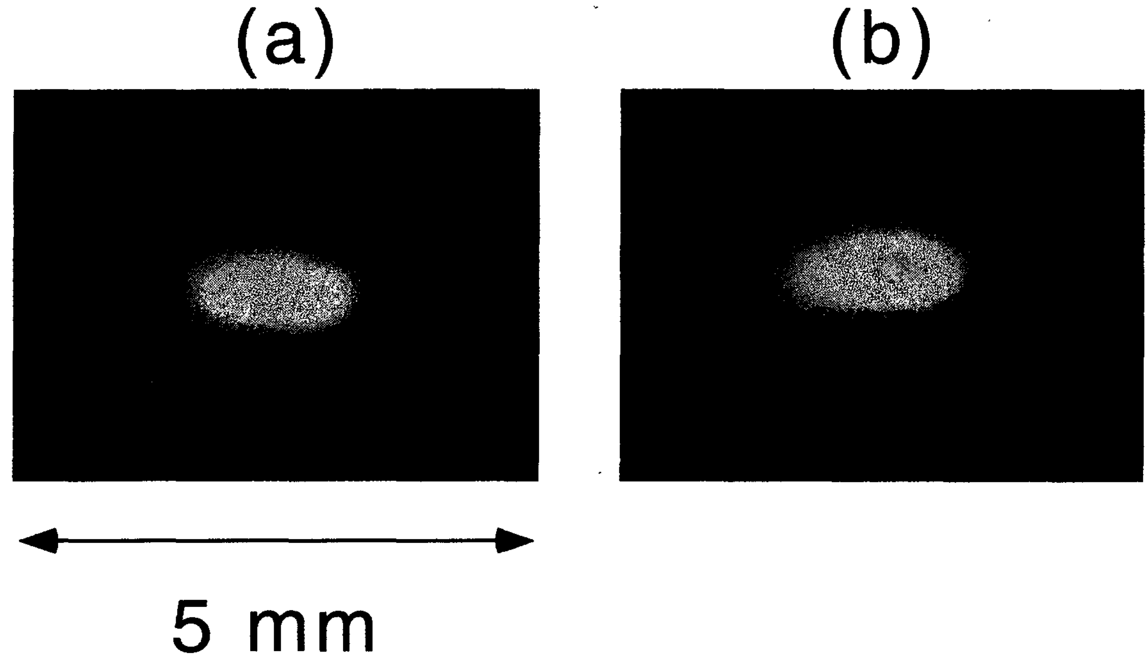

FIG. 2. Time integrated single shot OTR images at a fixed longitudinal position along the electron beam path in (a) vacuum, and (b) 4.1 Torr of laser ionized TPA. The images were obtained by imaging the OTR with a telescope on a cooled 16 bit CCD camera.

By integrating the total intensity from OTR recorded on the CCD camera and by measuring the beam charge with the ICT's before and after the plasma lens, respectively, we found that no charge was lost.

To study the effect of return current, the ratio of plasma skindepth to beam size was adjusted. This was accomplished by controlling the plasma density through the initial neutral gas pressure as well as the electron beam size at the entrance of the plasma lens, using conventional quadrupole magnets. The peak plasma densities for these two cases were 2.3×10^{13} cm^{-3} and 2.9×10^{14} cm^{-3}, corresponding to $k_p\sigma_r = 0.33$ and 1.1 and $k_p\sigma_z = 4.1$ and 12.3, respectively. The temporal plasma response was therefore adiabatic, which physically means that the current rise was slow compared to the plasma period. For each case, the electron beam size σ_r, time-integrated over the electron bunch, was measured as a function of propagation distance z using the scanning OTR system. Horizontal and vertical line profiles through the beam images were then fitted with a Gaussian distribution.

The evolution of the time-integrated transverse electron beam size σ_r versus z, was studied through an axisymmetric beam envelope model and a particle-in-cell code. Including only effects of the radial force due to the beam self-fields, plasma response and the beam emittance, the envelope equation for the azimuthally symmetric beam can be written as [17]

$$\frac{\partial^2\sigma_r}{\partial z^2} - \frac{\varepsilon^2}{\sigma_r^3} - \frac{1}{\gamma mc^2}\frac{< rW_r >}{2\sigma_r} = 0, \tag{1}$$

where $\sigma_r = \sqrt{< r^2/2 >}$, ε is the beam emittance ($\varepsilon = \varepsilon_x = \varepsilon_y$), γ is the relativistic factor, and no acceleration was assumed due to longitudinal wakefields (i.e. $\frac{\partial\gamma}{\partial z} = 0$). The radial wakefield can be written as [18,19]

$$W_r = 4\pi e^2[k_p \int_{-\infty}^{\xi} d\xi' \sin k_p(\xi - \xi')R(r, z, \xi') - \frac{1}{\gamma^2}R(r, z, \xi)], \tag{2}$$

with

$$R(r, z, \xi) = -k_p K_1(k_p r) \int_0^r r'dr' n_b(r', z, \xi) I_0(k_p r') + k_p I_1(k_p r) \int_r^\infty r'dr' n_b(r', z, \xi) K_0(k_p r'), \tag{3}$$

where $\xi = v_b t - z$ is the distance from the head of the bunch, v_b is the beam velocity in the z direction, and I_0, I_1, K_0 and K_1 are the modified Bessel functions. In the adiabatic limit and when the space charge field of the electron beam is cancelled by the plasma, the radial force W_r is due to the magnetic component of the Lorentz force ($v \times B$) and can be calculated from the electron beam and induced plasma return current $j_p(r)$:

$$W_r = -ev_b \frac{4\pi}{c^2 r} \int_0^r r'dr'(ev_b n_b(r') - j_p(r')). \tag{4}$$

To evaluate the average of the radial force, the beam density is assumed Gaussian

$$n_b(r, z, \xi) = \frac{N_b}{(2\pi)^(3/2)\sigma_r^2(z, \xi)} e^{-r^2/2\sigma_r^2(z,\xi) - \xi^2/2\sigma_z^2}, \tag{5}$$

where

$$< rW_r(r, z, \xi) >= \frac{1}{\sigma_r^2(z, \xi)} \int_0^\infty rdre^{-r^2/2\sigma_r^2} rW_r(r, z, \xi). \tag{6}$$

In the adiabatic limit, the return current can be calculated from [19]

$$j_p = v_b k_p^2 e \int_0^\infty r' dr' n_b(r', z, \xi) I_0(k_p r_<) K_0(k_p r_>). \tag{7}$$

where $k_p(z) = \omega_p(z)/v_b$ and $r_<(r_>)$ denotes the smaller (larger) of r and r'. The reduction in average focusing force as a function of $k_p\sigma_r$ is shown in Fig. 3. For the experimental parameters a reduction by about a factor 2 is expected in changing $k_p\sigma_r$ from 0.33 to 1.1.

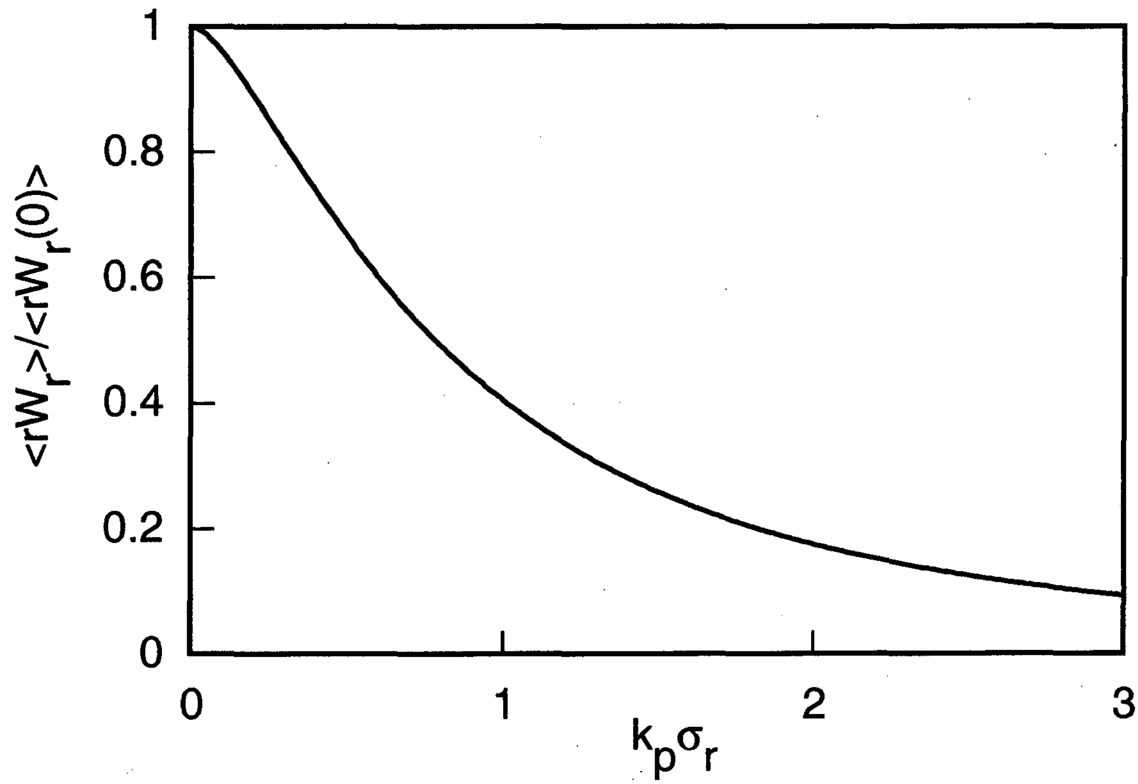

FIG. 3. Ratio of average force including return current effects to the average force in the absence of return currents as a function of $k_p\sigma_r$.

To model the experiment, the initial electron bunch was subdivided into independent longitudinal slices, each with a transverse size $\sigma_r = \sqrt{< r^2 > /2}$ and the envelope equation was solved for each slice. The resulting $\sigma_r(z, \xi)$ were averaged over the beam profile to obtain the beam size as

$$< \sigma_r(z) >= \frac{1}{\sqrt{2\pi}\sigma_z} \int_{-\infty}^{\infty} d\xi \sigma_r(z, \xi) e^{-\xi^2/2\sigma_z^2}. \tag{8}$$

To study the effect of the return current, the radial force was then evaluated using (a) the full expression (Eq. 2, 3), which includes the contribution to the magnetic field from both the return and beam currents and (b) using the focusing force due solely to the magnetic field of the beam, i.e. ignoring the return current contribution.

In addition to the envelope model, particle-in-Cell (PIC) simulations were performed using a $2^{1/2}D$ (two spatial dimensions r,z and three velocity components), fully electromagnetic and relativistic code XOOPIC [20]. The code includes space charge and boundary effects. The boundary condition was taken as a cylindrical conducting pipe with the radius much larger than the plasma size. The number of particles in the simulation was $4 \times 10^4 - 8 \times 10^4$ for the beam and $8 \times 10^4 - 4 \times 10^5$ for the plasma. To benchmark the code for beam - plasma systems, electromagnetic fields and electron beam propagation results were compared with known analytical expressions as well as with the envelope equation simulations and found to be in excellent agreement.

For the case where $k_p\sigma_r = 0.33$, Fig. 4(a), shows the measured as well as calculated rms beam envelope radius, including and ignoring the return current effect, versus longitudinal position. The experimental measurements are in good agreement with the results from the envelope and the particle-in-cell code XOOPIC, but cannot distinguish between the envelope model with or without the inclusion of the return current. Indeed, for this value of $k_p\sigma_r$, the predicted beam envelope calculated without return current differs only slightly from the results of a calcuation with return currents. Only about 12% of the return current flows within the rms beam area, resulting in a small reduction in focusing strength as seen in Fig. 3.

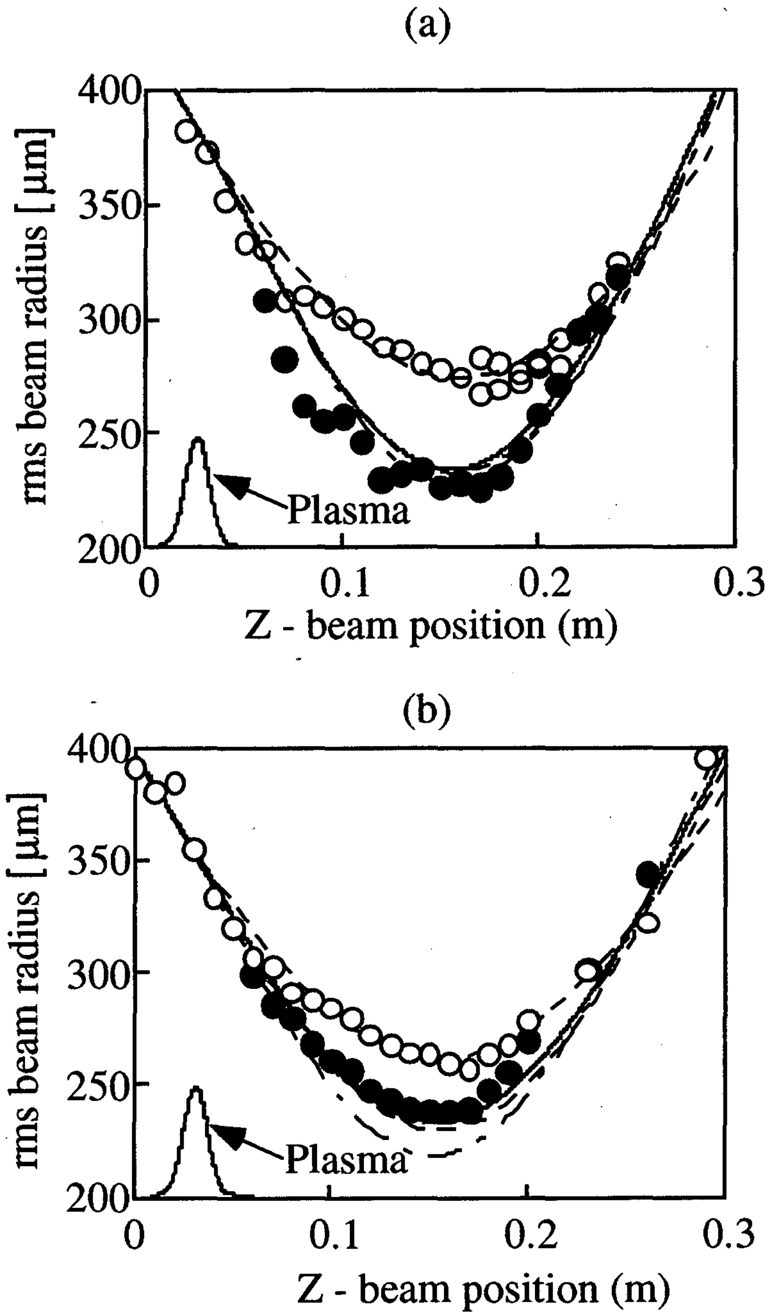

FIG. 4. Beam envelope measurement (dots) and simulation (lines), as a function of propagation distance, z for (a) $k_p\sigma_x = 0.33$ and (b) $k_p\sigma_x = 1.1$. Each dot represents an average of 10-20 shots. Solid curves are obtained using the code XOOPIC,dashed curves are obtained using the envelope equation for TPA (no laser) and overdense plasma and the dashed-dot curve is the result of the envelope model with return current off. A laser ionized plasma with density 2.3×10^{13} cm^{-3} for case (a) and 2.9×10^{14} cm^{-3} for case (b) is centered at $z = 4.4$ cm.

As seen in Fig. 4(b), for the case where $k_p\sigma_r = 1.1$, the experimental results and the beam envelopes obtained from simulations with XOOPIC are in very good agreement. However, as expected, good agreement between the measurements and the envelope model is only obtained when return currents are included. For this case, approximately 37% of the return current flows inside the rms beam area, causing a significant reduction in magnetic field and hence in the focusing strength (see Fig. 3).

We thank L. Archambault, J. Dougherty, W. Byrne, S. Wheeler, P. Volfbeyn and the ALS staff for their assistance with the experiment, M. Perry for the loan of the Nd:YAG laser, R. Stevens for the loan of the microwave interferometer, C.K. Birdsall and J. Verboncoeur for making XOOPIC available, and D. Whittum and E. Esarey for discussions on the envelope equations and return current physics.

REFERENCES

[1] For a recent review with many references see E. Esarey et al., IEEE Trans. Plasma Sci. **PS-24**, 252-288 (1996).

[2] P. Chen, Particle Accelerators **20**, 171 (1987).

[3] H. Murayama and M.E. Peskin, Annual Review of Nuclear and Particle Sciences **46**, 533 (1996).

[4] J.B. Rosenzweig et al.,Phys. Fluids B **2**, 1376 (1990); H. Nakanishi et al., Phys. Rev. Lett. **66**, 14 (1991); G. Hairapetian et al., Phys. Rev. Lett. **72**, 2403 (1995).

[5] N. Barov et al., Phys. Rev. Lett. **80**, 81 (1998).

[6] D.H. Whittum et al., Particle Accelerators **34**, 89 (1990).

[7] M.Tabak et al., Phys. Plasmas **1**, 1626 (1994); R.J. Mason and M. Tabak, Phys. Rev. Lett. **80**, 524 (1998).

[8] A. Pukhov and J. Meyer-ter-Vehn, Phys. Plasmas **5**, pp. 1880-1886 (1998).

[9] R. Govil, Ph.D. Thesis, UC Berkeley, 1998; R. Govil, S. Wheeler, W.P. Leemans, Proc. 1997 Part. Accel. Conf., 654 (1997).

[10] W. P. Leemans et al.,Proc.1993 Part. Accel. Conf., 83 - 85 (1993).

[11] W. P. Leemans,AIP Conference Proceedings **398**, 23 (1996).

[12] L. Wartski et al. J. Appl. Phys. **46**, 3644-53 (1975).

[13] P. Chen et al., Phys. Rev. Lett. **64**, 1231 (1990).

[14] T. Katsouleas and C.H. Lai, AIP Conference Proceedings **279**, 551 (1992).

[15] K. Oide, Phys. Rev. Lett. **61**, 1713 (1988).

[16] R. Govil, P. Volfbeyn, W.P. Leemans, Proc. 1995 IEEE Part. Accel. Conf., Dallas,Texas,

p. 776 (1995).

[17] E. P. Lee and R. K. Cooper, *Part. Accel.* **7**, 83 (1976)

[18] R. Keinigs and M. E. Jones, *Phys. Fluids* **30**, 252, (1987)

[19] E. Yu. Backhaus, D. Whittum and J. Wurtele, in preparation.

[20] J.P. Verboncoeur, A.B. Langdon and N.T. Gladd, Comp. Phys. Comm. **87**,199-219 (1995).

ERNEST ORLANDO LAWRENCE BERKELEY NATIONAL LABORATORY
ONE CYCLOTRON ROAD | BERKELEY, CALIFORNIA 94720

Prepared for the U.S. Department of Energy under Contract No. DE-AC03-76SF00098